RSC Advances

PAPER

View Article Online
View Journal | View Issue

Cite this: *RSC Adv.*, 2020, **10**, 16769

Conductive conduit small gap tubulization for peripheral nerve repair

Xingxing Fang,[abd] Jiuxu Deng,[cd] Wei Zhang,[ad] Haichang Guo,[b] Fei Yu,[ad] Feng Rao,[cd] Qicheng Li,[ad] Peixun Zhang,*[ad] Shulin Bai*[b] and Baoguo Jiang*[acd]

Received 7th March 2020
Accepted 1st April 2020

DOI: 10.1039/d0ra02143a

rsc.li/rsc-advances

Despite advances in surgical techniques, functional recovery following epineurial neurorrhaphy of transected peripheral nerves often remains quite unsatisfactory. Small gap tubulisation is a promising approach that has shown potential to traditional epineurial neurorrhaphy in the treatment of peripheral nerve injury. Thus, the goal of this study is to evaluate sciatic nerve regeneration after nerve transection, followed by small gap tubulization using a reduced graphene oxide-based conductive conduit. *In vitro*, the electrically conductive conduit could promote Schwann cell proliferation through PI3K/Akt signaling pathway activation. *In vivo*, the results of electrophysiological and walking track analysis suggest that the electrically conductive conduit could promote sensory and motor nerve regeneration and functional recovery, which is based on the mechanisms of selective regeneration and multiple-bud regeneration. These promising results illustrate electrically conductive conduit small gap tubulization as an alternative approach for transected peripheral nerve repair.

1. Introduction

Peripheral nerve injury is a common clinical disease, which always results in varying degrees of paralysis or sensory deficits.[1,2] However, the current treatment strategies are epineurial neurorrhaphy and lamellar sheath suture, which cannot achieve sufficient and accurate abutment of nerve fibers and resolve the problem of mismatch of sensory and motor nerve fibers.[3,4] Previous animal experiments and multi-center clinical trials have demonstrated that the repair effects of 2 mm small gap tubulization for peripheral nerve injuries are quite a bit better than those of traditional epineurial neurorrhaphy.[5,6] The 2 mm gap provides a suitable microenvironment for axons selective regeneration. Moreover, the conduit could prevent the escape of ruptured regenerating axons and reduce neuroma occurrence.[6] However, previous studies focus on surgery and biological researches, ignoring material improvement (only chitosan material).

The ability to conduct electricity is an essential aspect of synthetic nerve conduits due to the electrical signal exchange and conductive properties of nerve tissue.[7,8] In animal models and humans, electrical stimulation accelerates motor and sensory axon outgrowth across injury sites and enhances nerve regeneration and target reinnervation.[9,10] Thus, most studies about nerve tissue engineering have focused on conductive materials, hoping to develop a novel material that can meet both the conductivity demands of nerve tissue and the requirements of tissue engineering.

We have fabricated a novel conductive conduit containing gelatin methacryloyl (GelMA) and reduced graphene oxide (rGO) to repair critical peripheral nerve defects. Then, this work aims to investigate a electrically conductive conduit for peripheral nerve repair using a small gap sleeve bridging method.

2. Materials and methods

2.1. Fabrication of conductive nerve conduit and characterization

The conductive nerve conduit was synthesized and characterized as the previous report. Briefly, the rGO (0.25 and 0.5wt%) and trifluoroethanol (TFE) were mixed. The mixture was dispersed *via* probe ultrasonication for 30 min to obtain the uniform rGO solution. And a certain amount of GelMA/PCL (GelMA : PCL = 1 : 1 by weight) was added to produce the rGO/GelMA/PCL solution,[11] which was the mass ratio of the final mixture solution. The as-prepared solution was filled in a 10 ml syringe connected to a 21-gauge stainless steel needle, and then electrospun (IonBeam, WL-2C, China) applying at the constant parameters: UV light (0.5% w/v Irgacure 2959 as photoinitiator), 9 w; flow rate, 2 ml h^{-1}; the distance between needle tip to collector, 15 cm; supplied voltage, 15 kV; temperature, 30–40 °C; relative humidity, 30–40%. The collecting mandrel

[a]*Department of Orthopedics and Trauma, Peking University People's Hospital, Beijing, 100044, China. E-mail: jiangbaoguo@vip.sina.com; zhangpeixun@bjmu.edu.cn*

[b]*Department of Materials Science and Engineering, CAPT/HEDPS, Key Laboratory of Polymer Chemistry and Physics of Ministry of Education, College of Engineering, Peking University, Beijing, 100871, China. E-mail: slbai@pku.edu.cn*

[c]*Department of Trauma Medicine Center, Peking University People's Hospital, Beijing, 100044, China*

[d]*National Center for Trauma Medicine, China*

consisted of a stainless-steel rod with 1.2 mm, and the speed of the mandrel was 800 rpm. Finally, the obtained conductive conduits were subsequently dried in vacuum for at least 3 days, and then the stainless-steel rods were removed before use.

2.2. RSC96 culture and western blotting

The RSC96 seeded onto the nanofiber scaffolds (C group: 0 wt% rGO, A group: 0.25 wt% rGO, B group: 0.5 wt% rGO) at a density of approximately 1×10^4 cells per cm^2 and cultured in DEMEM medium with 10% fetal bovine serum and penicillin/streptomycin. RSC96 at the same density cultured on the tissue culture plate as control (Ctrl group).

After 3 days of culture, the cells were lysed in RIPA lysis buffer to collect total proteins. The total proteins were separated on SDS-PAGE gels and transferred to PVDF membranes. After blocking with 1% BSA for 1 h, the membranes were incubated at 4 °C overnight with the following primary antibodies: anti-p44/42 MAPK(ERK1/2) (1 : 2000, 4696, Abcam, USA), anti-Phospho-p44/42 MAPK(ERK1/2) (1 : 2000, 4370, Abcam, USA), anti-Akt (1 : 1000, 4691, Abcam, USA), anti- Phospho-Akt (1 : 2000, 4060, Abcam, USA), and anti-GAPDH (1 : 1000, Abcam, USA). The next day, the membranes were incubated with horseradish peroxidase-conjugated secondary antibodies (1 : 2500, ZB-5301 and ZB-5305, ZSGB-Bio, China) for 1 h at room temperature. Blots were then developed by an enhanced chemiluminescence western blotting detection kit (BioRad, Hercules,CA, USA).

2.3. Animal surgery

All animal procedures were performed in accordance with the Guidelines for Care and Use of Laboratory Animals of Peking University People's Hospital and approved by the Animal Ethics Committee of Peking University People's Hospital. The animals were randomly divided into 4 categories: (1) 0 wt% rGO, the rGO/GelMA/PCL nanofibers conduits group (Control group, $n = 8$); 2) 0.25 wt% rGO, the rGO/GelMA/PCL nanofibers conduits group (A-rGO group, $n = 8$); 3) 0.5 wt% rGO, the rGO/GelMA/PCL nanofibers conduits group (B-rGO group, $n = 8$); 4) traditional epineurial neurorrhaphy group (TEN group, $n = 8$). The surgical procedure was carried out as the previous report.[5,12]

Briefly, adult female rats (200–250 g, Sprague-Dawley rats) were induced to anesthetic depth with inhaled isoflurane at 5% and maintained at 1.5–2.0% isoflurane throughout the surgery. Then, a small incision was created in the right leg of the rat to expose the sciatic nerve, and surrounding muscles were detached with blunt dissection. Then, the nerve was transected at the center of the right thigh. The proximal and distal stumps of the injured nerve were directly sutured using a 10-0 nylon monofilament suture. Conductive nerve conduits sutured to the proximal and distal ends of the injured nerve with 10-0 nylon sutures, and 2 mm small gaps existed between the two ruptured stumps (Fig. 1). Finally, muscle soft tissue and skin were closed accordingly with 4-0 nylon sutures. Subsequent postoperative observations were made at week 12.

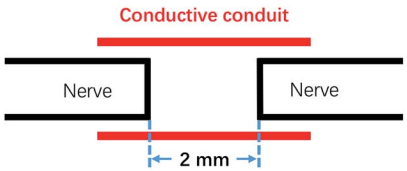

Fig. 1 Schematic of conductive conduit small gap tubulization methods. The gap between the nerve stumps is 2 mm.

2.4. Walking track analysis and electrophysiological assessment

The functional nerve recovery of the animals was assessed by Catwalk XT (Noldus, Catwalk XT, Netherlands) at 12 weeks after surgery. Briefly, the animals were allowed to walk on the walkway and carried out the data acquisition. A series of the landmarks of the footprints (for example, stand, max contact area, swing, duty cycle, the relative paw position) were analyzed.

After walking track analysis, SD rats were subjected to electrophysiological analysis. Under anesthesia conditions, the right sciatic nerve (operated nerve) and left nerve (non-operated nerve) was exposed. Bipolar electrodes were fixed at the proximal and distal part of the nerve to deliver single electrical signals. The recording electrodes placed in the tibialis anterior muscle. The various latency and distance between two ends of stimulation were recorded to measure compound muscle action potential (CMAP) and motor nerve conduction velocity (MNCV).

2.5. Muscles weight

At 12 weeks post operatively, tibialis anterior muscles and gastrocnemius muscles were harvested after SD rats were sacrificed. The relative weights were presented as percentages using previous studies: muscles weight% = (muscles weight of the operated leg)/(muscles weight of the unoperated leg). The experiment was repeated three times. The experiment was repeated eight times.

2.6. Statistical analysis

Unpaired Student's *t*-test and one-way ANOVA were used for statistical analysis. A *p*-value of less than 0.05 was considered statistically significant.

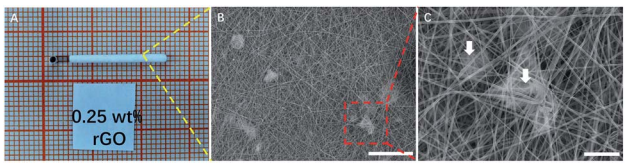

Fig. 2 (A) Image of conductive nerve conduits (rGO: 0.25 wt%). (B) Morphological photographs of conductive nerve conduits (rGO: 0.25 wt%). Scale bar = 50 μm. (C) is a magnified (B) image, white arrows indicate the rGO. Scale bar = 10 μm.

3. Results

3.1. Characterizations of conductive nerve conduits

As shown in Fig. 2. A, the electrically conductive nerve conduits were obtained by removing the stainless-steel rod and had an inner diameter of 1.2 mm with the wall thickness ~200 nm. SEM images of the conductive conduits are shown in Fig. 2B and C, the nanofibers and rGO were randomly oriented and formed a 3D interconnected porous structure. The conductive conduits were composed of fibers with diameters of approximately 310 nm.

3.2. Western blot

Phosphatidylinositol 3 kinase and protein kinase B (PI3K/Akt), and mitogen-activated protein kinase/extracellular signal-regulated kinase (MAPK/ERK) are common signaling pathways, which could regulate cell proliferation.[13,14] As shown in Fig. 3, the ratio of p-ERK/ERK among the A group, B group, and C group exhibited no significant difference. The ratio of p-ERK/ERK among the A group, B group, and C group was higher than that of the Ctrl group. However, the ratio of p-AKT/AKT in the A groups exhibited a marked increase compared with the Ctrl group, B group, and C group.

3.3. Animal surgery

All rats recovered from the surgeries and shown no wound complications and inflammatory signs. As shown in Fig. 4A1–D1, the conduits well integrated with the sciatic nerve, leaving a 2 mm gap for nerve regeneration. After 12 weeks of implantation (Fig. 4A2–D2), the conduits still appeared well integrated with the sciatic nerve and no apparent neuroma formation. Moreover, the conduits were not surrounded by a serious chronic inflammatory reaction and a thin layer of fibrous tissue abundant in capillaries.

3.4. Walking track analysis

To evaluate the recovery of nerve function, we carried out the walking track analysis. Proper walking depends on coordinated function involving sensory input, motor response, and cortical integration.[15] Moreover, walking track analysis provides a non-invasive method of evaluating the functional status of the sciatic nerve during the regeneration process. Stand is used in pain research and measures how much time the animal stands on one of its hind paws, which always affects max contact area. Swing Speed is the speed of the paw during Swing. Stand, SwingSeed, and max contact area depend on the pressure exerted by the paw during locomotion, which indirectly reflects mechanical allodynia.[15,16] As shown in Fig. 5A–C, compared with the Control group, A-rGO group and B-rGO group exhibited smaller mechanical allodynia. But, compared with the TEN group, the A-rGO group and B-rGO group exhibited lower

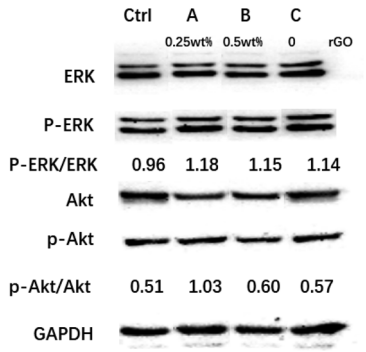

Fig. 3 Western blot analysis of ERK, p-ERK, Akt, and p-Akt expression after RSC96 co-cultures with scaffolds.

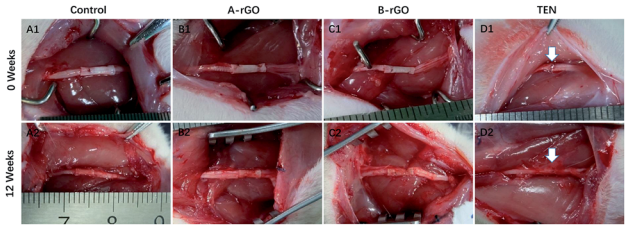

Fig. 4 Surgical implantation. (A1/2–D1/2) Intraoperative images of the Control group (A1/2), A-rGO group (B1/2), B-rGO group (C1/2), and TEN group (D1/2). White arrows indicate the end-to-end suture site.

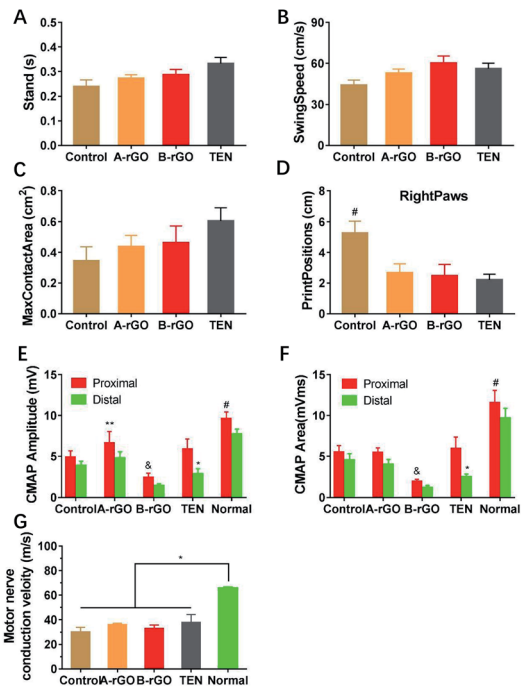

Fig. 5 Electrophysiology and walking track analysis. (A–D) Footprints and footfall patterns of Control group, A-rGO group, B-rGO group, and TEN group after 12 weeks of implantation, respectively. $^{\#}P < 0.05$. Error bar = s.e.m. (E and F) CMAP amplitudes and area of Control group, A-rGO group, B-rGO group, and TEN group. $^{*}P < 0.05$ between proximal and distal of the sciatic nerve. $^{**}P < 0.05$ between Control group and A-rGO group. $^{\&}P < 0.05$ between Control group and B-rGO group. $^{\#}P < 0.05$ between TEN group and other groups. Error bar = s.e.m. (G) Motor nerve conduction velocities of Control group, A-rGO group, B-rGO group, and TEN group. $^{*}P < 0.05$, Error bar = s.e.m.

mechanical allodynia. Generally, the rats tend to place their hind paw at the previous position of the forepaw. As shown in Fig. 5D, the PrintPosition of the TEN group, the A-rGO group, and the B-rGO group were significantly smaller compared with that of the Control group.

3.5. Electrophysiological assessment

To further evaluate the recovery of nerve function, we carried out the electrophysiological analysis, which is one of the most common parameters of functional recovery of the sciatic nerve regeneration.[17] The numbers of regenerated motor nerve fibers and the rate of muscle reinnervation could be indirectly reflected by compound muscle action potential (CMAP).[18,19] CMAP was evoked and recorded, followed by measurements of amplitude and area of signals. As shown in Fig. 5E and F, for proximal CMAP analysis, significance existed between the A-rGO, B-rGO, Control, and TEN groups. There were no significant differences between A-rGO and TEN groups. The proximal CMAP amplitude of the A-rGO group was more extensive than that of the Control group. More importantly, the proximal CMAP amplitude and area of the TEN group was significantly more significant than the distal CMAP amplitude and area of the TEN group, but this difference was not detected in the other groups.

In addition, motor nerve conduction velocity (MNCV) shows an essential index for the conduction function of the peripheral nerve, which indirectly reflects the fiber diameter, axon diameter, and myelin thickness of the regenerated nerve.[20] As shown in Fig. 5. G, there were no statistically significant differences among the B-rGO, A-rGO, Control, and TEN groups. The A-rGO group has similar MNCV compared to TEN group.

3.6. Muscle weight

To analysis the atrophy of the target muscles, the muscle weight was calculated. Generally, nerve dominates and feed its muscle and also receive muscle movement information. Then, muscle recovery can also indicate functional nerve recovery. At 12 weeks, we weighed and analyzed the muscles. As shown in Fig. 6, compared with contralateral muscle, affected muscle shown different degrees of atrophy. However, there was no difference between them.

4. Discussion

Unlike the central nervous system, the peripheral nerve has the ability for regeneration after injury.[21] The intrinsic and extrinsic promote the axon regenerate cross the injury sites and then rebuild functional connections with their original targets.[21,22] Generally, nerve transections destroy the continuity of the axons and nerve basal lamina, forcing a physical method to recover the continuity. Not surprisingly, the use of epineurial neurorrhaphy is the standard method for the repair of nerve transection in the clinic.[3] However, functional recovery following repair of transected nerves is even great challenges, owing to misdirection of the regeneration of the regenerating axons and a decreased number of axons.[23] Recently, 2 mm small gap

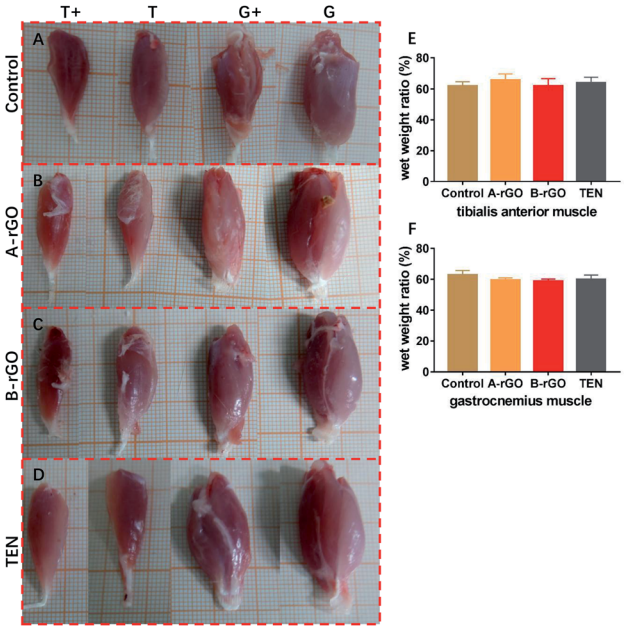

Fig. 6 Morphological photographs of muscles and wet muscles ratio. Morphological images of Control group (A), A-rGO group (B), B-rGO group (C) and TEN group (D), experimental side's tibialis anterior muscles (T+), contralateral side's tibialis anterior muscles (T), experimental side's gastrocnemius muscles (G+), contralateral side's gastrocnemius muscles (G). (E) and (F) The tibialis anterior muscles ratio and gastrocnemius muscle ratio. *P < 0.05. Error bar = s.e.m.

tubulization method has been applied in aminal models and human, and has excellent outcomes compared with traditional epineurial neurorrhaphy.[5,6] 2 mm small gap tubulization offers several advantages over traditional epineurial neurorrhaphy: (1) ready-to-use and fewer sutures cause less surgical trauma to the nerve stump; (2) less tension is applicated at the repair site; (3) prevent the escape of ruptured regenerating axons; (4) pre-customized for reducing the mismatch and allowing selective regeneration.[5,6,23,24]

Apart from the 2 mm small gap, the synthetic nerve guide tubes also play a critical role in nerve repair. Numerous studies have demonstrated that successful regeneration can take place across a gap that is bridged by artificial nerve guidance conduits.[8,25] With the development of technology, a wide range of biomaterials and techniques have been used to prepare nerve guidance conduits.[26] Graphene and its derivation have attracted great attention in the preparation of nerve guidance conduits because of their unique high electrical conductivity and the unique morphology of the rippled and wrinkled chemical surface, which mimics the surrounding matrix of neurons.[27,28] Previous studies verified that graphene-based scaffolds could elicit endogenous peripheral nerve repair mechanisms and successfully promote functional and morphological recovery in peripheral nerve regeneration.[12,29,30]

Bioelectricity and the existence of endogenous electric fields for tissue regeneration play an indispensable role in maintaining normal biological functions.[30] Conductive materials could meet both the electrical conductivity demands of nerve

tissue and the requirements of tissue engineering as a whole. In this work, we used a pre-customized graphene-based conductive nerve conduit as scaffolds to repair nerve transection (Fig. 2). The conductive nerve conduit well sutured in the sciatic nerve and successfully built a 2 mm gap. After 12 weeks of implantation, there was no complication occurs and the surface of the conduit existed connective tissues and blood vessels, which indicates that the conductive guidance conduit has excellent biocompatibility (Fig. 4).

Following a transection, the stump retracts, and the distal part of the nerve takes place Wallerian degeneration.[40] The major purpose of the regeneration process is for the axons to regrow back to their original targets.[31] Remarkably, previous work verified that the number of axons and Schwann cells at the axonal cross-section area was higher than that of the proximal end of the injured nerve, namely multiple-bud regeneration (multiple amplification).[32,33] The 2 mm small gaps construct a relatively closed microenvironment that was propitious to multiple-bud regeneration.[6,32] Moreover, graphene oxide could promote nerve-associated cells adhesion, proliferation, and differentiation.[29,34] Our work has shown that the conductive conduits could significantly activate PI3K/Akt signaling pathways, which was essential for Schwann cell proliferation (Fig. 3).[35,36]

After nerve transection, the Schwann cells from both the proximal and distal stump invade the bridge as multicellular cords and migrate directionally, eventually rejoining, which can provide a tube-like substrate to direct the regenerating axons back to their original targets.[31,37] Thus, Schwann cells proliferation coordinates with axons multiple-bud regeneration. CMAP indirectly reflects the numbers of regenerated motor nerve fibers, while MNCV indirectly reflects fiber diameter, axon diameter, and myelin thickness of the nerve.[18–20] The difference between proximal and distal CMAP of the TEN group has shown that some regenerated axons failed to select appropriate roads to back to their original targets. The proximal CMAP Amplitude of the A-rGO group was larger than the Control and B-rGO groups (Fig. 5E). Therefore, conductive conduits promote Schwann cell proliferation, thus regenerating axons have more "cellular conduits" to cross the injuries sites. After 12 weeks, based on the results from the walking track analysis, we found that the parameters of the A-rGO group was much better, which suggests that the electrically conductive conduits could improve the reconstruction of sensory function (Fig. 5A–D). Non-significant results do not mean that muscle weight does not work (Fig. 6). The main reason is the effect too small to detect.

5. Conclusion

In conclusion, we have demonstrated that rGO-based conductive nerve conduits, which fabricated by electrospinning, hold great promise for peripheral nerve repair by 2 mm small gaps tubulization method. Although electrical stimulation has been the most widely studied, which can significantly promote the regeneration of peripheral nerve injuries,[29,38,39] we have to point out that we do not apply electrical stimulation in this study. Thus, we will focus on the use of electrical stimulation in 2 mm small gaps rat models in future.

Conflicts of interest

There are no conflicts to declare.

Acknowledgements

The work was supported by Major R & D Program of National Ministry of Science and Technology (2018YFB1105504), National Natural Science Foundation (11672002, 31771322, 31571235, and 31571236), Beijing Municipal Science and Technology Commission Science and Technology Nova Cross Project (2018019), Ministry of Education Innovation Program of China (IRT16R01, IRT1201), Key Laboratory of Trauma and Nerve Regeneration, Ministry of Education (2018), National Center for Trauma Medicine, Peking University Medicine Seed Fund for Interdisciplinary Research supported by "the Fundamental Research Funds for the Central Universities"(BMU2018ME003), and Chinese National Ministry of Science and Technology 973 Project (2014CB542201). The authors would also like to thank Bin Fan (KYKY Technology CO., LTD.), Wenlong Li (KYKY Technology CO., LTD.), and Yingdong Li (Beijing Ion Beam Technology Co., Ltd.) for their time and effort in electrospinning and SEM tests.

References

1 L. Gu, [Construction of Chinese peripheral nerve society and progress in repair and reconstruction of peripheral nerve injury], *Zhongguo Xiufu Chongjian Waike Zazhi*, 2018, **32**(7), 786.
2 R. J. Duarte-Moreira, K. V. Castro, C. Luz-Santos, J. Martins, K. N. Sa and A. F. Baptista, Electromyographic Biofeedback in Motor Function Recovery After Peripheral Nerve Injury: An Integrative Review of the Literature, *Appl. Psychophysiol. Biofeedback*, 2018, **43**(4), 247.
3 T. Fujiwara, K. Matsuda, T. Kubo, K. Tomita, R. Hattori, T. Masuoka, K. Yano and K. Hosokawa, Axonal supercharging technique using reverse end-to-side neurorrhaphy in peripheral nerve repair: an experimental study in the rat model, *J. Neurosurg.*, 2007, **107**(4), 821.
4 R. S. Meyer, R. A. Abrams, M. J. Botte, J. P. Davey and S. C. Bodine-Fowler, Functional recovery following neurorrhaphy of the rat sciatic nerve by epineurial repair compared with tubulization, *J. Orthop. Res.*, 1997, **15**(5), 664.
5 P. Zhang, N. Han, T. Wang, F. Xue, Y. Kou, Y. Wang, X. Yin, L. Lu, G. Tian, X. Gong, S. Chen, Y. Dang, J. Peng and B. Jiang, Biodegradable Conduit Small Gap Tubulization for Peripheral Nerve Mutilation: A Substitute for Traditional Epineurial Neurorrhaphy, *Int. J. Med. Sci.*, 2013, **10**(2), 171.
6 P. Zhang, X. Yin, Y. Kou, N. Han, T. Wang, G. Tian, L. Lu and B. Jiang, Peripheral nerve mutilation through biodegradable conduit small gap tubulisation: a multicentre randomised trial, *Lancet*, 2015, 386S40.

7 M. Gajendiran, J. Choi, S. Kim, K. Kim, H. Shin, H. Koo and K. Kim, Conductive biomaterials for tissue engineering applications, *J. Ind. Eng. Chem.*, 2017, **51**, 12–26.
8 J. Xie, M. R. MacEwan, S. M. Willerth, X. Li, D. W. Moran, S. E. Sakiyama-Elbert and Y. Xia, Conductive Core-Sheath Nanofibers and Their Potential Application in Neural Tissue Engineering, *Adv. Funct. Mater.*, 2009, **19**(14), 2312.
9 T. Gordon, Electrical Stimulation to Enhance Axon Regeneration After Peripheral Nerve Injuries in Animal Models and Humans, *Neurotherapeutics*, 2016, **13**(2), 295.
10 K. M. Chan, M. W. Curran and T. Gordon, The use of brief post-surgical low frequency electrical stimulation to enhance nerve regeneration in clinical practice, *J. Physiol.*, 2016, **594**(13), 3553.
11 X. Fang, J. Xie, L. Zhong, J. Li, D. Rong, X. Li and J. Ouyang, Biomimetic gelatin methacrylamide hydrogel scaffolds for bone tissue engineering, *J. Mater. Chem. B*, 2016, **4**(6), 1070.
12 Y. Qian, J. Song, X. Zhao, W. Chen, Y. Ouyang, W. Yuan and C. Fan, 3D Fabrication with Integration Molding of a Graphene Oxide/Polycaprolactone Nanoscaffold for Neurite Regeneration and Angiogenesis, *Adv. Sci.*, 2018, **5**(4), 1700499.
13 R. Li, Y. Li, Y. Wu, Y. Zhao, H. Chen, Y. Yuan, K. Xu, H. Zhang, Y. Lu, J. Wang, X. Li, X. Jia and J. Xiao, Heparin-Poloxamer Thermosensitive Hydrogel Loaded with bFGF and NGF Enhances Peripheral Nerve Regeneration in Diabetic Rats, *Biomaterials*, 2018, 16824.
14 B. Li, T. Qiu, K. S. Iyer, Q. Yan, Y. Yin, L. Xie, X. Wang and S. Li, PRGD/PDLLA conduit potentiates rat sciatic nerve regeneration and the underlying molecular mechanism, *Biomaterials*, 2015, 5544.
15 L. Sarikcioglu, B. M. Demirel and A. Utuk, Walking track analysis: an assessment method for functional recovery after sciatic nerve injury in the rat, *Folia Morphol.*, 2009, **68**(1), 1.
16 E. A. Kappos, P. K. Sieber, P. E. Engels, A. V. Mariolo, S. D'Arpa, D. J. Schaefer and D. F. Kalbermatten, Validity and reliability of the CatWalk system as a static and dynamic gait analysis tool for the assessment of functional nerve recovery in small animal models, *Brain and Behavior*, 2017, **7**(7), e723.
17 N. Hu, H. Wu, C. Xue, Y. Gong, J. Wu, Z. Xiao, Y. Yang, F. Ding and X. Gu, Long-term outcome of the repair of 50 mm long median nerve defects in rhesus monkeys with marrow mesenchymal stem cells-containing, chitosan-based tissue engineered nerve grafts, *Biomaterials*, 2013, **34**(1), 100.
18 F. Mohamadi, S. Ebrahimi-Barough, M. R. Nourani, K. Mansoori, M. Salehi, A. A. Alizadeh, S. M. Tavangar, F. Sefat, S. Sharifi and J. Ai, Enhanced sciatic nerve regeneration by human endometrial stem cells in an electrospun poly(ε-caprolactone)/collagen/NBG nerve conduit in rat, *Artif. Cells, Nanomed., Biotechnol.*, 2018, **46**(8), 1731.
19 M. Wolthers, M. Moldovan, T. Binderup, H. Schmalbruch and C. Krarup, Comparative electrophysiological, functional, and histological studies of nerve lesions in rats, *Microsurgery*, 2005, **25**(6), 508.
20 S. G. Waxman, Determinants of conduction velocity in myelinated nerve fibers, *Muscle Nerve*, 1980, **3**(2), 141.
21 Z. He and Y. Jin, Intrinsic Control of Axon Regeneration, *Neuron*, 2016, **90**(3), 437.
22 F. Bradke, J. W. Fawcett and M. E. Spira, Assembly of a new growth cone after axotomy: the precursor to axon regeneration, *Nat. Rev. Neurosci.*, 2012, **13**, 183–193.
23 R. S. Meyer, R. A. Abrams, M. J. Botte, J. P. Davey and S. C. Bodine Fowler, Functional recovery following neurorrhaphy of the rat sciatic nerve by epineurial repair compared with tubulization, *J. Orthop. Res.*, 1997, **15**(5), 664.
24 P. X. Zhang, A. Li-Ya, Y. H. Kou, X. F. Yin, F. Xue, N. Han, T. B. Wang and B. G. Jiang, Biological conduit small gap sleeve bridging method for peripheral nerve injury: regeneration law of nerve fibers in the conduit, *Neural Regener. Res.*, 2015, **10**(1), 71.
25 W. Jing, Q. Ao, L. Wang, Z. Huang, Q. Cai, G. Chen, X. Yang and W. Zhong, Constructing conductive conduit with conductive fibrous infilling for peripheral nerve regeneration, *Chem. Eng. J.*, 2018, 345566.
26 M. D. Sarker, S. Naghieh, A. D. McInnes, D. J. Schreyer and X. Chen, Regeneration of peripheral nerves by nerve guidance conduits: influence of design, biopolymers, cells, growth factors, and physical stimuli, *Prog. Neurobiol.*, 2018, 171125.
27 X. Liu, A. L. Miller, S. Park, B. E. Waletzki, Z. Zhou, A. Terzic and L. Lu, Functionalized Carbon Nanotube and Graphene Oxide Embedded Electrically Conductive Hydrogel Synergistically Stimulates Nerve Cell Differentiation, *ACS Appl. Mater. Interfaces*, 2017, **9**(17), 14677.
28 S. R. Shin, Y. C. Li, H. L. Jang, P. Khoshakhlagh, M. Akbari, A. Nasajpour, Y. S. Zhang, A. Tamayol and A. Khademhosseini, Graphene-based materials for tissue engineering, *Adv. Drug Deliv. Rev.*, 2016, **105**(pt B), 255.
29 J. Wang, Y. Cheng, L. Chen, T. Zhu, K. Ye, C. Jia, H. Wang, M. Zhu, C. Fan and X. Mo, In vitro and in vivo studies of electroactive reduced graphene oxide-modified nanofiber scaffolds for peripheral nerve regeneration, *Acta Biomater.*, 2019, 8498.
30 R. Geetha Bai, N. Ninan, K. Muthoosamy and S. Manickam, Graphene: a versatile platform for nanotheranostics and tissue engineering, *Prog. Mater. Sci.*, 2018, 9124.
31 A. Cattin, J. J. Burden, L. Van Emmenis, F. E. Mackenzie, J. J. A. Hoving, N. Garcia Calavia, Y. Guo, M. McLaughlin, L. H. Rosenberg, V. Quereda, D. Jamecna, I. Napoli, S. Parrinello, T. Enver, C. Ruhrberg and A. C. Lloyd, Macrophage-Induced Blood Vessels Guide Schwann Cell-Mediated Regeneration of Peripheral Nerves, *Cell*, 2015, **162**(5), 1127.
32 Z. Peixun, H. Na, Y. Kou, Y. Xiaofeng and B. Jiang, Peripheral nerve intersectional repair by bi-directional induction and systematic remodelling: biodegradable conduit tubulization from basic research to clinical application, *Artif. Cells, Nanomed., Biotechnol.*, 2017, **45**(8), 1464.

33 G. J. Bao, F. Y. Xiao, D. Y. Zhang, G. F. Zhong and B. Z. Hong, Maximum Number of Collaterals Developed by One Axon during Peripheral Nerve Regeneration and the Influence of That Number on Reinnervation Effects, *Eur. Neurol.*, 2007, **58**(1), 12–20.

34 J. Song, H. Gao, G. Zhu, X. Cao, X. Shi and Y. Wang, The preparation and characterization of polycaprolactone/graphene oxide biocomposite nanofiber scaffolds and their application for directing cell behaviors, *Carbon*, 2015, 951039.

35 B. He, S. Liu, Q. Chen, H. Li, W. Ding and M. Deng, Carboxymethylated chitosan stimulates proliferation of Schwann cells in vitro via the activation of the ERK and Akt signaling pathways, *Eur. J. Pharmacol.*, 2011, **667**(1–3), 195.

36 S. Chattopadhyay and V. I. Shubayev, MMP-9 controls Schwann cell proliferation and phenotypic remodeling via IGF-1 and ErbB receptor-mediated activation of MEK/ERK pathway, *Glia*, 2009, **57**(12), 1316.

37 M. P. Clements, E. Byrne, L. F. Camarillo Guerrero, A. Cattin, L. Zakka, A. Ashraf, J. J. Burden, S. Khadayate, A. C. Lloyd, S. Marguerat and S. Parrinello, The Wound Microenvironment Reprograms Schwann Cells to Invasive Mesenchymal-like Cells to Drive Peripheral Nerve Regeneration, *Neuron*, 2017, **96**(1), 98.

38 J. Senger, V. Verge, H. Macandili, J. L. Olson, K. M. Chan and C. A. Webber, Electrical stimulation as a conditioning strategy for promoting and accelerating peripheral nerve regeneration, *Exp. Neurol.*, 2017, 30275.

39 A. Mendez, H. Seikaly, V. L. Biron, L. F. Zhu and D. W. Cote, Brief electrical stimulation after facial nerve transection and neurorrhaphy: a randomized prospective animal study, *Journal of Otolaryngology – Head & Neck Surgery*, 2016, **45**, 7.

40 Zochodne and W. Douglas, Early regenerative events, *Neurobiology of Peripheral Nerve Regeneration*, Cambridge UK, 2008, pp. 58–84.